Proapoptotic effects of *P. aeruginosa* involve inhibition of surfactant phosphatidylcholine synthesis

Florita C. Henderson,[1,*,] Olga L. Miakotina,[1,*,**] and Rama K. Mallampalli[2,*,†,§,**]**

Departments of Internal Medicine* and Biochemistry,† the Department of Veterans Affairs Medical Center,§ and Roy J. and Lucille A. Carver College of Medicine,** The University of Iowa, Iowa City, IA 52242

Abstract ***Pseudomonas aeruginosa*** **causes sepsis-induced acute lung injury, a disorder associated with deficiency of surfactant phosphatidylcholine (PtdCho).** ***P. aeruginosa*** **(PA103) utilizes a type III secretion system (TTSS) to induce programmed cell death. Herein, we observed that PA103 reduced alveolar PtdCho levels, resulting in impaired lung biophysical activity, an effect partly attributed to caspase-dependent cleavage of the key PtdCho biosynthetic enzyme, CTP:phosphocholine cytidylyltransferase-α (CCTα). Expression of recombinant CCTα variants harboring point mutations at putative caspase cleavage sites in murine lung epithelia resulted in partial proteolytic resistance of CCTα to PA103. Further, caspase-directed CCTα degradation, decreased PtdCho levels, and cell death in murine lung epithelia were lessened after exposure of cells to bacterial strains lacking the TTSS gene product, exotoxin U (ExoU), but not ExoT. These observations suggest that during the proapoptotic program driven by** ***P. aeruginosa*****, deleterious effects on phospholipid metabolism are mediated by a TTSS in concert with caspase activation, resulting in proteolysis of a key surfactant biosynthetic enzyme.**—Henderson, F. C., O. L. Miakotina, and R. K. Mallampalli. **Proapoptotic effects of** ***P. aeruginosa*** **involve inhibition of surfactant phosphatidylcholine synthesis.** ***J. Lipid Res.*** **2006.** 47: **2314–2324.**

Supplementary key words apoptosis • caspase • Pseudomonas

Pseudomonas aeruginosa is a Gram-negative bacterium that can cause sepsis, particularly in immunocompromised individuals. *P. aeruginosa* is also a well-recognized nosocomial pathogen etiologically linked to high morbidity and mortality attributed to acute pulmonary exacerbations. This organism is the predominant isolate in nosocomial pneumonia (1) and cystic fibrosis (2), and is the predominant organism in sepsis-associated acute lung injury or the acute respiratory distress syndrome (3). Several characteristics of *P. aeruginosa* represent unique challenges to its effective treatment. The organism secretes multiple virulence factors, is genetically flexible, and triggers an exuberant host response (2). Major virulence factors include alginate, exotoxin A (ExoA), and quorum sensing for biofilm generation and numerous other soluble products (2). In particular, *P. aeruginosa* encodes a type III secretion system (TTSS) that confers high-level virulence, allowing the bacterium to induce eukaryotic cell injury (4). This system is comprised of an array of bioeffector molecules, translocators, and ExsA, a transcriptional activator of the TTSS regulon (5). To date, four type III effectors have been identified: ExoS, ExoU, ExoT, and ExoY. ExoS and ExoT have 75% primary sequence identity, functioning as ADP-ribosyltransferases, and encode a GTPase-activating protein activity (6–8). ExoY is an adenylate cyclase, and ExoU exhibits phospholipase A_2 activity (8, 9).

One mechanism whereby *P. aeruginosa*-derived toxins might initiate or accentuate acute lung injury is by decreasing surfactant, a complex surface-active material enriched with dipalmitoylphosphatidylcholine (DPPC) and key proteins that stabilize alveoli (10). In this regard, *P. aeruginosa* degrades surfactant apoproteins involved in bacterial clearance (11–13). *P. aeruginosa* also decreases surfactant phospholipid levels in several animal models, although the mechanisms are not known (14–19). It is plausible that *P. aeruginosa* might accelerate DPPC breakdown, because ExoU exhibits phospholipase activity (14, 20). However, our recent studies and studies by others indicate that lipase inhibition alone fails to restore surfactant levels after *P. aeruginosa* infection (14). These observations suggest other complementary mechanisms whereby the pathogen might perturb surfactant synthesis or secretion, leading to respiratory impairment.

The synthesis of phosphatidylcholine (PtdCho) and DPPC in the lung occurs via the CDP-choline pathway (10). The rate-regulatory enzyme within this synthetic pathway is CTP:phosphocholine cytidylyltransferase (CCT) (21). CCTα, unlike CCTβ isoforms also described, is the pre-

Manuscript received 30 June 2006 and in revised form 24 July 2006.

Published, JLR Papers in Press, July 25, 2006.
DOI 10.1194/jlr.M600284-JLR200

Abbreviations: CCT, CTP:phosphocholine cytidylyltransferase; CPT, cholinephosphotransferase; DPPC, dipalmitoylphosphatidylcholine; Exo, exotoxin; LDH, lactate dehydrogenase; PARP, poly (ADP-ribose) polymerase; PtdCho, phosphatidylcholine; TTSS, type III secretion system.

[1] F. C. Henderson and O. L. Miakotina contributed equally to this work.
[2] To whom correspondence should be addressed.
e-mail: rama-mallampalli@uiowa.edu

dominant isoform in pulmonary tissues. The enzyme contains 367 residues that map within four functional regions, incuding a catalytic core, amino-terminal nuclear localization and membrane binding domains, and a carboxyl-terminal phosphorylation domain (22). Recently, we demonstrated that *P. aeruginosa* infection rapidly (within 1 h) activates calcium-activated neutral proteases that degrade CCTα, leading to reduced DPPC levels in bronchoalveolar lavage (23). However, *P. aeruginosa* also activates caspases during late-phase bacterial-induced programmed cell death (4). Caspase degradation of CCTα occurs as a long-term effect of cytotoxic drugs during apoptosis (24). In the process of investigating *P. aeruginosa* signaling, we observed a late-phase response whereby the pathogen triggers programmed cell death in pulmonary epithelia. These observations led us to hypothesize that *P. aeruginosa*-induced programmed cell death in surfactant-producing alveolar epithelial cells is ExoU specific and associated with caspase-driven hydrolysis of CCTα, leading to decreased DPPC biosynthesis. Herein, we show that this hypothesis was confirmed, inasmuch as pathogen signaling involves both exoenzymes or exotoxins and proteinases that impair surfactant synthesis.

MATERIALS AND METHODS

Materials

The murine lung epithelial (MLE-12) cell line was obtained from American Type Culture Collection (ATTC; Manassas, VA). DMEM/F-12 and DMEM (Dulbecco's modified Eagle's medium) were obtained from the University of Iowa tissue culture and hybridoma facility (Iowa City, IA). The Western blotting detection (SuperSignal ELISA Femto) and B-PER 6×His purification kit were purchased from Pierce Biotechnology (Rockford, IL). The rabbit polyclonal antibody against poly (ADP-ribose) polymerase (PARP) was obtained from Cell Signaling Technology, Inc. (Danvers, MA). QuikChange II site-directed mutagenesis kit was purchased from Stratagene (La Jolla, CA), and human recombinant caspases were obtained from Biomol International (Plymouth Meeting, PA). TNT T7 Coupled Reticulocyte Lysate System was purchased from Promega (Madison, WI). Redivue L-[^{35}S]methionine was from Amersham Biosciences. [1,2,3-^{3}H]glycerol was obtained from American Radiolabeled Chemicals, Inc. (St. Louis, MO). Tri reagent and protease inhibitor cocktail were purchased from Sigma-Aldrich (St. Louis, MO). The caspase inhibitor III was obtained from Calbiochem (La Jolla, CA). Complete Mini (protease inhibitor) was purchased from Roche (Mannheim, Germany). SYBR Green PCR master mix was obtained from Applied Biosystems (Foster City, CA). For animal studies, male C57BL/6J, 6–8 week-old mice, 20–25 g, were obtained from Jackson Laboratories (Bar Harbor, ME), and male 7–8 week-old, 200 g Sprague Dawley rats were obtained from Harlan (Indianapolis, IN). All experimental procedures involving mice and rats were performed in accordance with the protocols approved by the University of Iowa animal care and use committee.

Bacterial strains and preparation

P. aeruginosa (PA103) and PA103 mutants were kindly provided by Dr. Tim Yahr (University of Iowa, Iowa City, IA). PA103 was maintained in Vogel-Bonner minimal agar. Cultures were plated and grown overnight from frozen stock. Overnight plate cultures were then inoculated in tryptic soy broth supplemented with 1% glycerol and 100 mM sodium glutamate (TSB++) and grown by rotary shaking at 37°C to log phase, i.e., until the cultures achieved an optical density of 0.65–0.7 using A_{540}. A_{540} $1 = 1.37 \times 10^9$ colony-forming units/ml. In caspase inhibitor studies, colonies were scraped from the agar plate and suspended in TSB ++ and used directly for infection. The PA103 mutants used are described in **Table 1**.

Murine infection, cell isolation, and biophysical analysis

Mice were deeply anesthetized using ketamine (80–100 mg/kg i.p.) and xylazine (10 mg/kg i.p.) and intratracheally injected with buffer (control diluent) or *P. aeruginosa* (PA103). After 1 h, mice were euthanized with pentobarbital (150 mg i.p.), the lungs were lavaged, and surfactant pellets were isolated as described (25). Murine or rat primary alveolar type II epithelia were isolated as described (25).

In separate studies, mice were placed after infection on a FlexiVent ventilator (Scireq; Montreal, Quebec, Canada) using module 1 with a maximal stroke volume of 0.9 ml. Quasi-static ventilation was initiated using a tidal volume of 8.5 ml/kg and a rate of 150 breaths/min. The mice were paralyzed with 1 mg/kg of pancuronium bromide. The end expiratory pressure (PEEP) was adjusted to 1, 3, 5, 7, 9, and 11 cm PEEP prior to a series of maneuvers that were performed by the ventilator. The pressure in the ventilator cylinder that was used to deliver the breath and the volume of the breath were measured and used to calculate the lung pressure-volume relationships and elastance. Calculations were performed using the standard algorithms that were included in the FlexiVent Version 4 software program.

Cell culture and infection

Primary mouse or rat type II cells were cultured overnight in DMEM containing 10% carbon-stripped FBS for further analysis the next day. Prior to infection, cells were rinsed in antibiotic-free medium. MLE cells were maintained in Hite's medium with 2% FBS with antibiotics (100 μg/ml streptomycin and 100 U/ml penicillin) at 37°C in an atmosphere containing 5% CO_2. After reaching confluence, cells were harvested using 0.25% trypsin with 0.1% EDTA and seeded at a density of 1.5×10^6 cells/60 mm dish for use in experiments. After cells were incubated overnight at 37°C and 5% CO_2 and reached 80–85% confluence, the medium was changed to 2 ml fresh Hite's medium without antibiotics at least 1–3 h prior to infection. Cells were infected with wild-type PA103 or PA103 mutants at a multiplicity of infection (MOI) of 1–50 for 3–4 h in the dose-response studies. Cells were harvested once morphological signs of apoptosis (i.e., rounding of cells, shrinking of cell membrane) were microscopically observed. For inhibitory studies, a caspase III inhibitor (5–80 μM) was added 30 min prior to PA103 infection. Trypan Blue staining

TABLE 1. PA103 mutants

PA103	Wild type
PA103ΔExoU	PA103 mutant lacking ExoU
PA103ExoT::Tc	PA103 mutant lacking ExoT
PA103ExsA::Ω	PA103 mutant defective in the expression of type III secretion genes
PA103ΔExoU ExoT::Tc.	PA103 mutant defective in production of both ExoU and ExoT

:: Ω, Insertion of tetracycline-resistant cassette gene; Δ, gene deletion; Exo, exotoxin. :: Tc, insertion of tetracycline-resistant cassette gene.

was performed to confirm percentage of cell death. Briefly, cells were trypsinized and stained with 0.4% Trypan Blue, then loaded into the hemacytometer (Neubauer) and counted.

Lipid analysis

PtdCho biosynthesis was measured as the rate of incorporation of [^{3}H]glycerol into PtdCho. Cells were pulsed with 12–50 μCi/2 ml medium of [1,2,3-^{3}H]glycerol to determine the rate of incorporation of the radiolabel into PtdCho and other phospholipids. Lipids were extracted using hexane-isopropanol-water (300:200:10), resolved by TLC using LK5D plates (Silica gel 150 A). Radioactivity within individual lipids was quantified by TLC scanner or scintillation scanner (Liquid Scintillation Analyzer, Packard). Levels of PtdCho and DPPC mass were measured using a phosphorus assay as described (26).

Enzyme assays

CCT activities were determined by measuring the rate of incorporation of [methyl-^{14}C]phosphocholine into CDP-choline using a charcoal extraction method (26). No lipid activator was added to the reaction mixture. Cholinephosphotransferase (CPT) activity was assayed as described (26).

Immunoblotting

MLE cells were harvested in lysis buffer (10 mM Tris HCl, pH 7.4, 150 mM NaCl, 1 mM EDTA, 1 mM EGTA, 1.5 mM $MgCl_2$, 50 mM NaF, 5 mM sodium pyrophosphate, 0.2 mM sodium orthovanadate, 10% glycerol, 1% Triton X-100, 0.5% Nonidet P-40, and Complete Mini protease inhibitor cocktail). Cellular extracts were sonicated and centrifuged. Equal amounts of protein cell lysates (30 μg) were resolved by SDS-PAGE on 10–15% gels, and immunoblots were probed for CCTα and PARP using polyclonal antibodies at dilutions of 1:2,000 or 1:1,000, respectively. The blots were subsequently developed by chemiluminescence. All membranes were stripped and reprobed for β-actin to confirm equal loading of proteins.

Lactate dehydrogenase assay

Lactate dehydrogenase (LDH) activity was measured in medium as a decline in NADH during conversion of pyruvate into lactate detected at 340 nm.

Construction of CCT mutants

GraBCas software was utilized to identify putative caspase cleavage sites within the CCTα primary sequence (27). Rat CCTα in pCMV5-CCTα-His (GenBank accession number, NM_078622) was mutated within predicted caspase cleavage sites at aspartate residues using site-directed mutagenesis. The resulting mutant plasmids were sequenced for confirmation. The following primers were used to mutate aspartic acid (D) to asparagine (N): CCTD28N, 5′ CTAATGGAGCAACAGAGGAA**A**ATGGAATTCCTTCCAAAG 3′; CCTD54N, 5′ TCTGATGAAATTGAAGTT**A**ACTTTAGTAAGCC-CTATGTCAGG 3′. Mutated nucleotides are shown in bold.

Quantitative PCR

Cells were collected in Tri reagent, and total RNA was isolated. Four micrograms of total RNA was subjected to DNA digest and reverse transcribed. Levels of mRNA were estimated by real-time PCR using primers for CCTα and mouse GAPDH as an internal control, and SYBR Green PCR master mix. CCTα primers used in the PCR assay mixture were the following: forward, 5′ cctggaaatgtttggtccaga 3′ and reverse, 5′ ctctgcttgggactgatgg 3′. Data were expressed relative to levels in control cells at 3 h of infection.

In vitro transcription and translation and caspase digestion of CCTα

For in vitro synthesis of CCTα mutants, cDNA constructs cloned into pCR4-TOPO4 (1 μg plasmid/reaction) were added directly to the rabbit reticulocyte lysate (TNT coupled reticulocyte lysate system) and incubated with T7 RNA polymerase in a 50 μl reaction containing [^{35}S]methionine (45 μCi/reaction) for 90 min at 30°C according to the manufacturer's instructions. Caspase digestions were performed with 6 μl of CCTα translation mixtures and 300 units of either caspase-6 or -8 in buffer (250 mM HEPES, 250 mM NaCl, 50 mM DTT, 50 mM EDTA, 25% glycerol, and 0.1% CHAPS) for 3 h at 30°C. One unit of human recombinant caspase activity is defined as 1 pmol/min at 30°C with tetrapeptide colorimetric substrate. Assays were terminated by the addition of protein sample buffer, heated to 90°C for 20 min and resolved in 12.5% SDS-PAGE.

CCTα purification

His-tagged purification was performed according to the manufacturer's instructions (Pierce Biotechnology). Briefly, cells were collected in mammalian lysis buffer with protease inhibitors (1:100; Sigma) and centrifuged at 14,000 *g* for 5 min. An equal amount of cell lysate (1.25 mg) was incubated with nickel-chelated agarose. His-tagged proteins were eluted, and concentrated using Millipore centricon YM-30 according to the manufacturer's instructions. Three micrograms of His-purified proteins was resolved by 12.5% SDS-PAGE.

Transfectional analysis

For overexpression of CCTα-full-length (CCTα-FL) and CCTα mutant plasmids (CCTD28N, CCTD54N), cells were transfected with CCTαFL-His, CCTD28N, and CCTD54N at 10 μg per 100 mm dish using Fugene 6 (Roche). After 4–6 h, medium was changed to Hite's medium with 1% FBS overnight, and cells were harvested and replated into 12-well dishes overnight. Cells were subsequently infected with PA103 (MOI = 5) and labeled with 10 μCi/well of [1,2,3-^{3}H]glycerol for 4 h for radiolabeled incorporation into PtdCho.

Statistical analysis

Statistical significance was accepted at the $P < 0.05$ level by *t*-test or one-way ANOVA for multiple group analysis with a Bonferroni adjustment.

RESULTS

PA103 infection impairs lung biophysical properties

Mice were infected with PA103 at an inoculum of 10^5 to 10^6. An hour after infection, the mice were euthanized and lungs were lavaged. PA103 decreased DPPC, the major surface-active phospholipid in lavage, by 60% versus control (**Fig. 1A**). These biochemical alterations induced by the bacterium were coupled to impairment of lung biophysical activity (Fig. 1B, C). Pulmonary compliance measurements in mice revealed a decrease in compliance, evidenced by a greater amount of pressure required to achieve a similar change in lung volume ($\Delta V/\Delta P$) in the group of mice infected with PA103 (Fig. 1B). Accordingly, the infected group showed a significant increase in lung

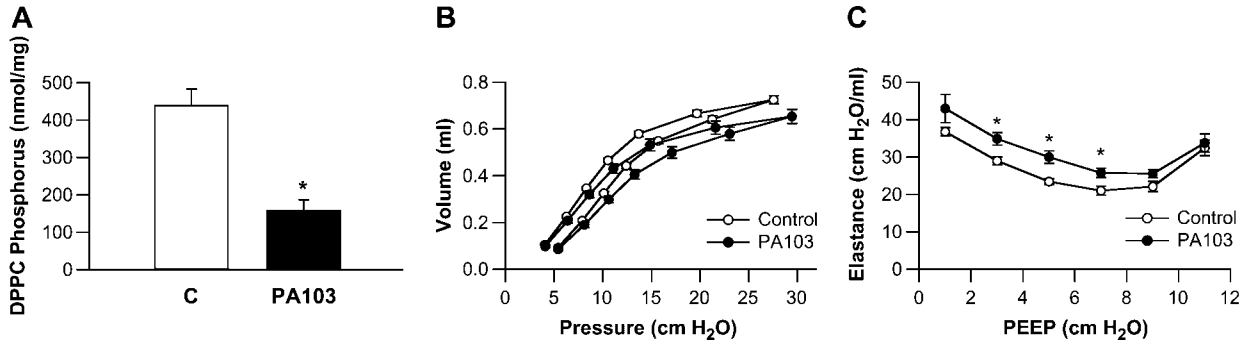

Fig. 1. PA103 infection lowers dipalmitoylphosphatidylcholine (DPPC) in lavage and impairs lung biophysical properties. C57BL/6J mice were intratracheally administered either buffer (control) or PA103 at an inoculum of 10^5 (A) or 10^6 (B, C) bacteria/mouse. After 1 h, mice were euthanized, the lungs were lavaged, and surfactant pellets were isolated. A: Surfactant pellets were analyzed for DPPC levels, expressed as nmol lipid phosphorus/mg protein. $^*P < 0.05$ versus controls (*t*-test, n = 4–7 animals). B: Control and PA103-infected mice were anesthesized, paralyzed, and mechanically ventilated with end expiratory pressure (PEEP)-3, and a quasi-static pressure/volume was measured using a Flexivent system. C: Elastance was also determined. The data are from n = 8 in control and n = 5 in the PA103-infected group. $^*P < 0.05$ versus controls (*t*-test). Data is presented as mean ± SEM.

elastance, a marker of pulmonary stiffness over a broad range of applied PEEP (Fig. 1C).

PA103 infection inhibits PtdCho synthesis

To determine whether decreased lavage DPPC levels after PA103 infection could be attributed to reduced synthesis of phospholipid, we performed pulse-labeling studies. In murine type II primary alveolar epithelial cells infected in vitro, PA103 significantly decreased [^{3}H]glycerol incorporation into PtdCho by nearly 40% (**Fig. 2A**). Compared with primary epithelia, MLE cells exhibited a more sensitive response to effects of PA103, but this occurred after more-prolonged exposure to the pathogen (3 h, MOI = 5). At 1 h, PA103 reduced PtdCho synthesis by ~30% (data not shown), and after a 3 h bacterial infection, a 70–80% decrease in labeling was observed (Fig. 2B). These effects were not associated with alterations in phosphatidylethanolamine synthesis (Fig. 2B). Dose-response analysis revealed that incorporation of [^{3}H]glycerol into PtdCho exhibited a dose-dependent decrease in radiolabeled activity after bacterial infection in MLE cells (Fig. 2C). The results demonstrate that PA103 decreases PtdCho synthesis in both mouse primary cells and a murine lung epithelial cell line, although the kinetics of these effects differ somewhat. These effects of PA103 on surfactant lipid synthesis in vitro may contribute to lower surfactant levels and impairment of lung function as observed in vivo.

Additional studies demonstrated that PA103 produced a dose-dependent decrease in CCT activity and CCTα mass in primary rat alveolar epithelial cells infected with PA103 (**Fig. 3A, B**). However, PA103 did not alter the activity of CPT, the final enzyme in the PtdCho biosynthetic pathway (Fig. 3A, inset). Additional studies with MLE cells revealed

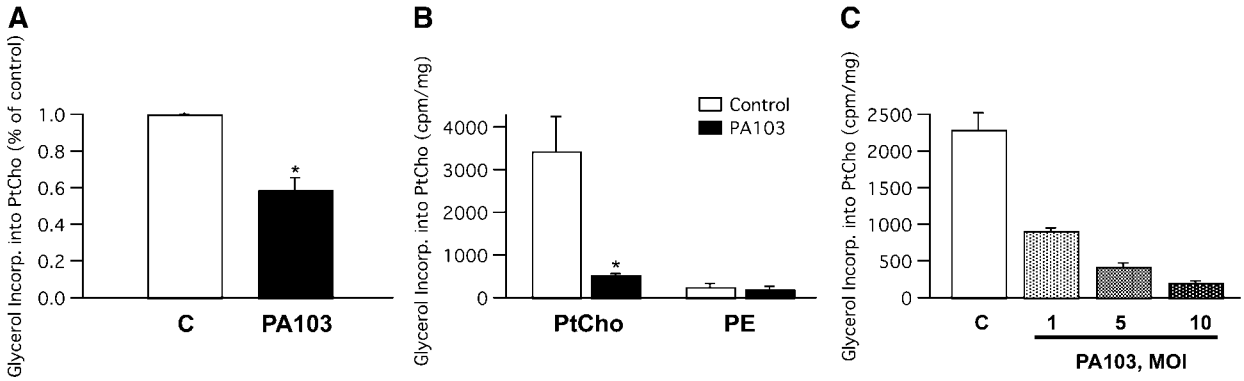

Fig. 2. PA103 infection inhibits de novo synthesis of phosphatidylcholine (PtdCho) in lung epithelia. Primary mouse alveolar type II cells and murine lung epithelial (MLE) cells were labeled with [^{3}H]glycerol and infected with PA103 at different multiplicities of infection (MOI) and for various times. A: Isolated primary type II cells were labeled with [^{3}H]glycerol (50 μCi/2 ml for 3 h) and infected with PA103 (MOI = 5) for 1 h. Data normalized to controls (C = 1) were obtained from type II cells isolated from 26 animals (means ± SEM). $^*P < 0.05$ versus controls, n = 3, *t*-test. B, C: MLE cells were labeled with [^{3}H]glycerol (12 μCi/2 ml) and infected with PA103 (MOI = 5) for 4 h (B) or with various MOIs of PA103 for 4 h (C). In each panel, after labeling, cells were harvested, and total cellular lipids were extracted and processed for radiolabeled incorporation of [^{3}H]glycerol into PtCho or phosphatidylethanolamine. In B, data represent three experiments (means ± SEM). $^*P < 0.05$ versus controls, *t*-test. In C, data from two experiments are expressed as means ± SD.

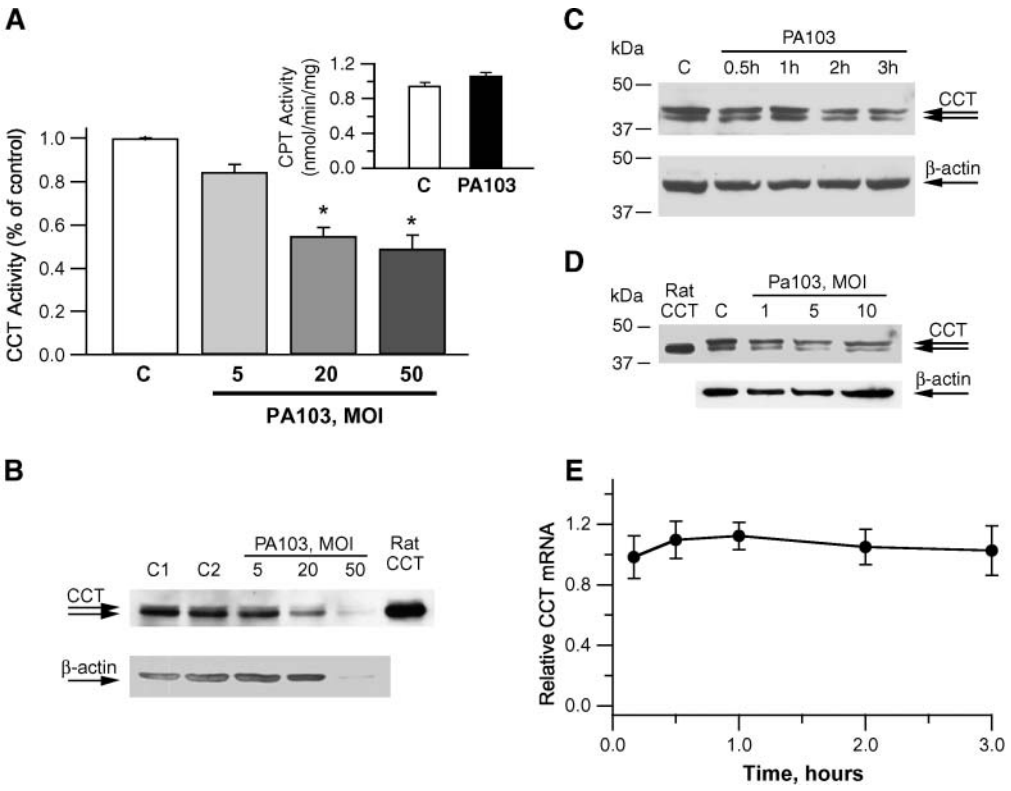

Fig. 3. PA103 degrades CTP:phosphocholine cytidylyltransferase-α (CCTα). A: Primary rat alveolar type II cells were infected with PA103 in vitro at various MOIs for 1 h, cells were harvested, and CCT activity or cholinephosphotransferase (CPT) activity [inset] was assayed. Data on CCT activity are expressed as the percent of control and are from type II cells isolated from n = 6 rats (n = 3 experiments, means ± SEM); $^*P < 0.05$ versus controls, ANOVA. CPT activity was measured in n = 2 rats in triplicate (means ± SEM). B: Primary rat alveolar type II cells infected with PA103 from studies in A were processed for immunoblotting for CCTα (above) and β-actin (below). C, D: MLE cells were infected with PA103 for various times at an MOI = 5 (C) or at various MOIs for 3–3.5 h (D) and subsequently harvested and processed for immunoblotting for CCTα (above) and β-actin (below). Panels C and D are representative blots from at least n = 3 independent experiments. E: Steady-state CCTα mRNA was determined by real-time PCR after various times of PA103 infection (MOI = 5). Total RNA was extracted, and quantitative PCR was performed using 4 μg of total cellular RNA. Data were normalized to levels of GAPDH mRNA (as an internal control) and expressed as fold stimulation over noninfected controls at 3 h. Data represent three individual experiments. Data bars represent mean ± SEM.

that PA103 also decreased enzyme levels in a dose- and time-dependent manner (Figs. 3C, D). In these experiments, CCTα was often detected as two predominant bands at ~42 kDa, probably representing phosphoCCTα variants, as described previously (24). However, CCTα mRNA levels remained unchanged during the PA103 infection at MOI = 5 (Fig. 3E). Thus, Pseudomonas infection in lung epithelia regulates CCTα at the posttranscriptional level. Overall, these data suggest that PA103 infection could inhibit PtdCho production by a decrease in levels of the rate-limiting enzyme in the PtdCho biosynthetic pathway.

PA103 induces apoptosis in pulmonary epithelia

Thus far, the data suggest that in murine lung cells, long-term exposure (>3 h) to PA103 exerts deleterious effects on surfactant phospholipid metabolism. We next investigated whether these effects may be linked to the apoptotic program. To determine whether PA103 induces apoptosis in mouse epithelial cells, cells were infected at MOI = 5 for up to 4 h. After infection, the media was collected for LDH release. We observed a modest increase in LDH release within 2 h and a progressive increase in LDH activity in medium over the next 2 h (**Fig. 4A**). Cellular lysates were subjected to gel electrophoresis and probed with polyclonal antibodies to PARP, a 116 kDa caspase-sensitive nuclear polymerase involved in DNA repair. PARP cleavage by caspases signifies cellular disassembly and serves as a marker for cellular apoptosis. As shown in Fig. 4B, PARP cleavage was detected within cells as early as 2 h after infection, evidenced by the appearance of the 89 kDa cleavage product. Thus, the coordinate release of LDH and cleavage of PARP in MLE cells in response to PA103 infection signal that events involved in apoptosis and cytotoxicity are well under way.

To determine the possible role of caspases in PA103-induced CCTα degradation, we pretreated cells with a broad-spectrum caspase inhibitor, caspase inhibitor III, to prevent CCTα cleavage. In these studies, PA103 induced a

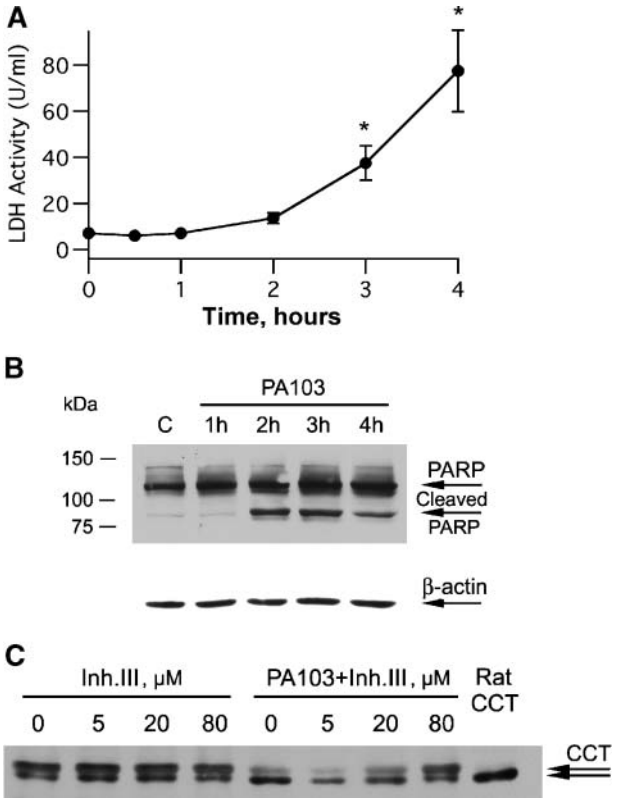

Fig. 4. PA103 infection induces apoptosis in MLE cells. A: MLE cells were infected with PA103 (MOI = 5) for up to 4 h, and medium was collected for analysis of lactate dehydrogenase (LDH) activity. Data are from three to five experiments, means ± SEM; $*P < 0.05$ versus controls, ANOVA. B: MLE cells were infected (MOI = 5) at indicated times. Cell lysates (40 μg) were subjected to gel electrophoresis and probed with poly (ADP-ribose) polymerase (PARP) (above) and β-actin (below) antibodies. C: MLE cells were preincubated with 5–80 μM of caspase inhibitor III for 30 min prior to infection with PA103 at MOI = 5 for 3 h. Cells were then harvested and processed for CCTα immunoblotting. The immunoblot represents one of three independent experiments.

shift, with a decrease in intensity of the upper band to a more predominant lower band, suggestive of CCTα dephosphorylation, as has been described after farnesol exposure (24). Indeed, levels of both CCTα bands were partially restored after incubation with 20 μM to 80 μM of the inhibitor in the presence of PA103 (Fig. 4C). These observations with pharmacological inhibition of caspase activity and CCTα cleavage were partial at log phase bacterial growth and more pronounced using PA103 during stationary growth. Thus, inhibitory effects of PA103 infection on CCTα protein stability and surfactant PtdCho synthesis may be partly attributed to caspase activation during the initial phases of the apoptotic program.

Caspases cleave CCTα

To examine the molecular basis whereby caspases might degrade CCTα, we performed in vitro caspase digestions. Analysis by GraBCas software identified several potential caspase attack sites at aspartate residues within the CCTα amino-terminal and catalytic domains (**Fig. 5A**). Proteolysis reactions using partially purified rat liver CCTα as a substrate and recombinant caspases-6 and -8 resulted in an uncleaved CCTα (42 kDa) and a ~37 kDa hydrolysis product (Fig. 5B). Caspase-9 also partially cleaved CCTα into a smaller fragment at ~32 kDa (Fig. 5B). On the basis of the size of the resulting hydrolysis products observed in Fig. 5B, we predicted that the D28 and D54 sites within the NH_2-terminal domain serve as potential targets for caspase cleavage of CCTα. Thus, these residues (D28 and D54) were mutated to asparagine by site-directed mutagenesis. These cDNA constructs, along with wild-type CCTα, were then directionally cloned into pCR4-TOPO4 and utilized in an in vitro transcription and translation system using ^{35}S-labeled methionine. Newly synthesized ^{35}S-labeled full-length and mutant CCTαs were then subjected to caspase-6 proteolysis, reaction products were resolved by SDS-PAGE, and autoradiography was performed. Radiography revealed that caspase-6 cleaved wild-type CCTα, resulting in the appearance of at least two breakdown products at ~39 kDa and 37 kDa. The CCTD28N mutant was significantly less sensitive to the effects of caspase; the intensity of the 42 kDa product was comparable to that of the wild-type CCTα, with minimal appearance of cleavage products. In addition, the CCTD54N mutant exhibited only partial caspase-6 resistance; a band of intermediate size (~39 kDa) was detected (Fig. 5C). Similar results were observed using caspase-8 proteolysis of CCTα (data not shown).

To examine in vivo sensitivities of these CCTα variants to bacterial infection, MLE cells were transfected, with His-tagged CCT plasmids encoding these proteins, cells were subsequently treated with or without PA103, cellular lysates were harvested, and CCTα was purified using a nickel column. As expected, compared with untransfected cells, CCTα levels increased significantly after transient transfection of various plasmids (**Fig. 6A**). Immunoblotting for CCTα in total cell lysates (containing both endogenous and overexpressed CCTα) revealed that PA103 infection produced variable levels of reduction of the ~42 kDa enzyme (Fig. 6A). However, immunoblotting for CCTα after His purification of cellular lysates, corrected for loading on our nickel column (Fig. 6B, upper panel), revealed that CCTα levels were indeed higher in cells expressing the proteolytically resistant CCTD28N plasmid after PA103 infection than in controls (Fig. 6B, lower panels). These data indicate that a pool of cells that express CCTα variants with mutations at caspase cleavage sites may be less vulnerable to caspase-driven proteolysis in response to bacterial infection.

We next examined whether expression of CCTα mutants in MLE cells leads to higher levels of radiolabeled incorporation of [^{3}H]glycerol into PtdCho after PA103 infection. In these experiments, we transfected cells with CCTα mutants and infected cells with or without PA103 the next day, followed by [^{3}H]glycerol labeling. As shown in Fig. 6C, analysis of radioactivity within PtdCho in untransfected cells revealed a ~60% reduction in synthesis of the phospholipid after PA103 infection compared with uninfected cells. Moreover, when analysis was assessed in transfected cells, PA103 decreased PtdCho synthetic rates

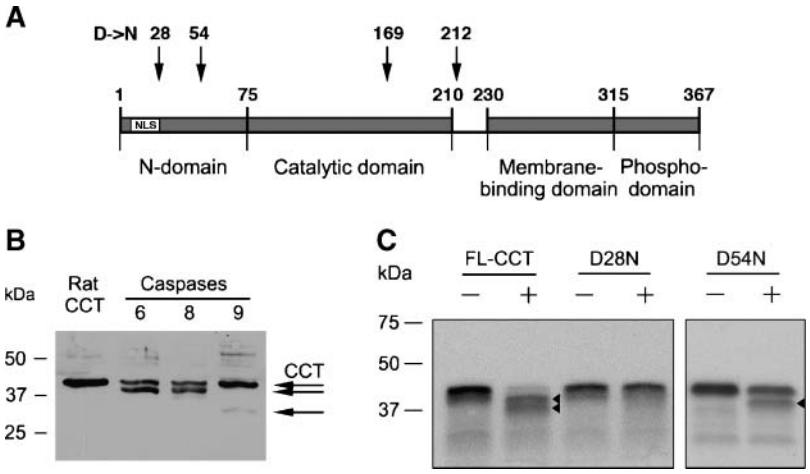

Fig. 5. In vitro digestion of CCTα by caspases. A: Schematic diagram of the CCTα functional domains showing putative caspase cleavage sites as indicated by arrows. B: Purified rat liver CCTα (5 μg) was reacted with 600 units of caspase-6, -8, and -9 at 37°C for 3 h. The reactions were terminated, and the products were resolved in a 12.5% SDS-PAGE gel and probed with an anti-rabbit CCTα antibody (n = 3). C: In vitro-translated ^{35}S-labeled CCTα and CCTα mutants were incubated with 300 units of human recombinant caspase-6 at 30°C for 3 h, resolved by SDS-PAGE, and processed for autoradiography. Blots represent five individual experiments.

by ~25–35% versus control (Fig. 6C). Collectively, these results demonstrate that overexpression of CCTα caspase-resistant mutants can partially attenuate the adverse effects of PA103 on CCTα degradation and surfactant lipid synthesis in lung epithelia.

PA103 regulation of PtdCho levels and apoptosis is TTSS dependent

The deleterious effects of PA103 in murine lung cells may be attributed to its TTSS (6). To determine bacterial factors that might mediate inhibition of phospholipid synthesis and drive apoptosis within murine lung epithelia, we used various PA103 mutants. These mutants are defective in elaboration of either the type III secretion apparatus (ExsA), ExoT, or ExoU, or harbor deletion of both ExoU and ExoT. Bacterial concentrations per dish were measured by optical density (OD_{540}) to confirm rates of bacterial growth per condition. As previously shown, MLE cells infected with wild-type PA103 (MOI = 5) showed a significant increase in LDH release by 4 h (Figs. 4A, **Fig. 7A**). Interestingly, cells infected with the PA103 mutants at MOI = 5 showed near-control LDH values (Fig. 7A). However, under these conditions, the ExoT mutant, compared with other mutants, displayed much slower growth rates, which may have led to lower LDH values. The growth of the ExoT mutant varied and appeared to be comparable to the growth rate of wild-type PA103 at MOI = 5 when added at MOI = 25–150. Thus, when infected at increasing MOI, the defective ExoT mutant also produced significant increases in LDH activity, suggesting that ExoU alone or in combination with other factors induces cytotoxicity (Fig. 7B). Figure 7C shows cleavage of PARP in MLE cells infected with wild-type PA103, the PA103 ExoU or Exo T mutants, and uncleaved PARP in control cells and in cells infected with the ExsA or double mutant (ExoU/ExoT). These observations indicate that early events within the apoptotic program are induced by ExoT and ExoU, whereas significant cytotoxicity in lung epithelia is driven by ExoU. Studies were next extended to analyze effects of PA mutants on CCTα levels. CCTα immunoblots revealed a significant decrease in steady-state CCTα levels after wild-type PA103 infection, but remarkably, levels of the enzyme were variably higher in cells after infection with all PA103 mutants except the ExoT mutant (Fig. 7D). Last, we assessed effects of individual PA mutants on PtdCho content (Fig. 7E). Indeed, PA103 decreased PtdCho mass by 25% ($P < 0.05$ vs. control); because this change represents a decrease in steady-state mass of the major phospholipid in cells rather than a measure of PtdCho synthetic rate, it is physiologically significant. In contrast, individual PA mutants did not significantly alter PtdCho levels in lung epithelia, with the exception of the ExoT mutant (Fig. 7E). These observations suggest that in addition to inducing cytotoxicity, ExoU within the TTSS is a major factor inhibiting PtdCho content.

DISCUSSION

A key feature of bacterial pathogens is their ability to disrupt membrane phospholipid integrity during programmed cell death (28, 29). These studies demonstrate for the first time that during the apoptotic program in pulmonary epithelia, a virulent strain of *P. aeruginosa* inhibits PtdCho synthesis via caspase-dependent cleavage of a key enzyme required for phospholipid synthesis. The unique findings from our studies include: *i*) that *P. aeruginosa* triggers site-specific proteolytic cleavage of the CCTα enzyme, which could result in decreased PtdCho synthesis; *ii*) that deleterious effects of the pathogen on

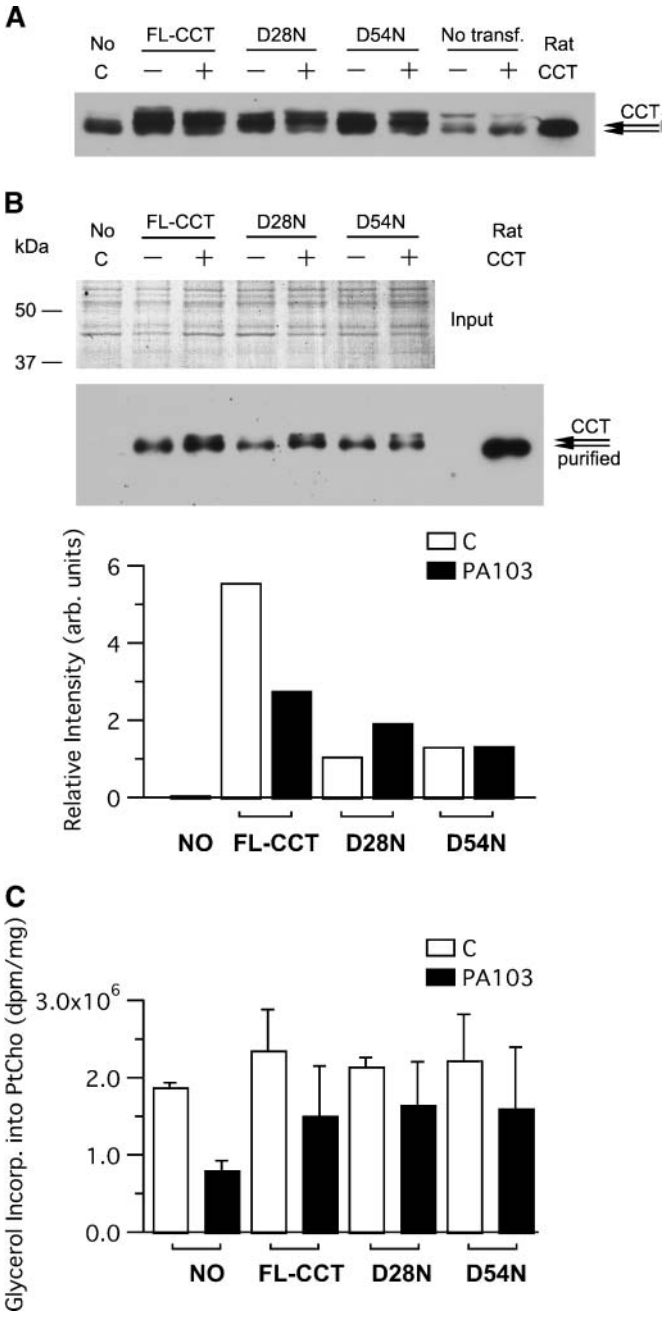

Fig. 6. CCTα caspase mutants exhibit partial resistance to PA103 degradation. A, B: MLE cells were transiently transfected with full-length CCTα (FL-CCT) or one of two His-tagged CCTα plasmids harboring mutations at putative caspase cleavage sites within the NH_2-terminal domain (D28N and D54N). The following day, cells were infected with or without PA103, and cell lysates were harvested. Some of the cellular extracts were processed for CCTα purification on a nickel column. The cell lysates (A) and His-purified CCTα mutants (3 μg) (B) were subjected to immunoblotting with a CCTα antibody. Prior to application to the column, the His-purified proteins were subjected to Coomassie Blue staining (B, top input). Densitometric measurements (B, bottom) were performed for the 45–60 kDa region. The blots represent two individual experiments. C: MLE cells were transiently transfected with CCTα and CCTα mutant plasmids. The transfectants were then labeled with [^{3}H]glycerol with or without PA103 (MOI = 5) for 4 h. Cells were then processed for [^{3}H]glycerol incorporation into PtdCho. Data are from two experiments (means ± SD).

CCTα breakdown are partially reversed with either caspase inhibition or expression of CCTα mutants where caspase attack sites were modified; and *iii*) that the TTSS, specifically ExoU, serves as a critical virulence factor that targets the PtdCho biosynthetic pathway. The results suggest that interventions designed to manipulate either the bacterial components (e.g., exotoxins) or host response (e.g., CCTα) within lipogenic pathways might be important in lessening the severity of injury observed after pulmonary infection with *P. aeruginosa*.

There is currently a paucity of data on the molecular mechanisms whereby bacteria modulate PtdCho synthesis. *P. aeruginosa* secretes enzymes that exhibit phospholipase A_2-like activity, and indeed, this may be a contributing mechanism during the early phases of bacterial infection (20, 30). *Streptococcus pneumoniae* initiates apoptosis in neuronal cells and A549 cells, the latter a transformed airway epithelial cell line, via inhibition of PtdCho synthesis (29). However, these effects appear to be due to inhibition of the activity of CPT, the terminal enzyme within the PtdCho synthetic pathway (29). Other noninfectious, pro-apoptotic agents also decrease CPT activity, leading to inhibition of PtdCho synthesis (24, 31). *P. aeruginosa* did not alter CPT activity in the present study, indicating that mechanisms for this pathogen are distinct.

Our recent studies show that *P. aeruginosa* depletes lavage DPPC levels, an effect associated with cleavage of the CCTα enzyme (23). However, these effects of the pathogen were rapid (1 h), were mediated partly by calcium-activated neutral proteinases (calpains), and occurred before the onset of programmed cell death (Fig. 4). Importantly, adenoviral gene transfer of calpain-resistant CCTα mutants attenuated the inhibitory effects of *P. aeruginosa* on lavage DPPC levels (23). These observations led us to investigate long-term (>2 h) responses of alveolar epithelia to bacterial infection, where we observed a robust inhibitory effect of *P. aeruginosa* on PtdCho synthesis. During this period, PA103 infection reduced immunoreactive CCTα levels without alterations in steady-state CCT mRNA, suggestive of reduced enzyme protein stability. These changes were linked to initiation of the apoptotic program, evidenced by cleavage of PARP, partial reversal of CCTα degradation by caspase inhibition, and disruption of cellular membrane integrity. Of note, the kinetics for decreased PtdCho synthesis in response to PA103 preceded activation of programmed cell death, because PtdCho synthesis was reduced within 1 h prior to stimulation of PARP cleavage. These findings, together with those of others, suggest that bacterial inhibition of PtdCho synthesis may be an important contributor to programmed cell death (29).

A hallmark of apoptotic cell death is the activation of caspases. Chemotherapeutic agents trigger caspase activation and apoptosis in lung epithelia (32). Lagace, Miller, and Ridgway demonstrated that caspases cleave CCTα in response to farnesol, an isoprenoid chemotherapeutic agent (24). Consistent with their studies, we show that caspases-6 and -8 clearly cleave CCTα to ~37 and 39 kDa fragments. Caspases-6 and -8 have two common attack sites within the CCTα NH_2-terminal domain, at TEED^{28}G and

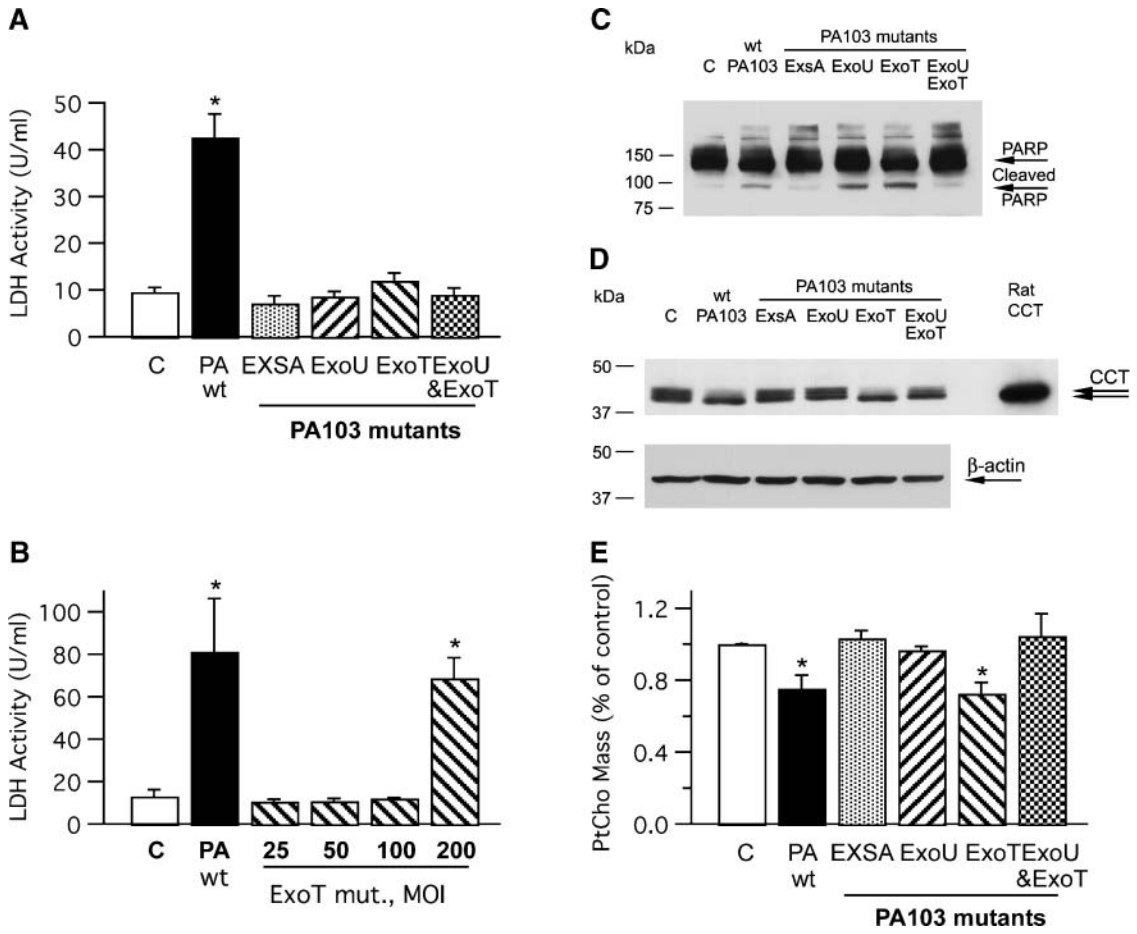

Fig. 7. PA103-induced programmed cell death is type III secretion system (TTSS) dependent. A: MLE cells were infected with wild-type PA103 and various PA103 mutants (MOI = 5) for 4 h. Mutants with defective expression of either the TTSS gene (ExsA), exotoxin U (ExoU), or ExoT, or mutants harboring a double mutation with deletion of both ExoU and ExoT were used in experiments. The growth rates of mutants, with the exception of the ExoT mutant, were comparable to that of wild-type PA103 under these conditions. Cells were exposed to mutants, and culture medium was collected for LDH activity. Data are presented as means ± SEM; $*P < 0.05$ versus controls, ANOVA, n = 4. B: Because the ExoT mutant exhibited slower growth rates compared with other mutants, cells were infected with increasing MOIs of the ExoT mutant, and LDH activity was assayed as in A. Data are from two to three experiments and are presented as means ± SD. $*P < 0.05$ versus controls, ANOVA, n = 3. C, D: MLE cells were infected with wild-type PA103 and other PA103 mutants at MOI = 5 and with ExoT mutant at MOI = 50 for 3 h, and lysates were processed for PARP (C), CCTα, and β-actin immunoblotting (D). E: MLE cells were infected as above at MOI = 5 for PA103 and other mutants and MOI = 25 for the ExoT mutant for 3 h. PtdCho mass was quantitatively analyzed by phosphorus assay. Data represent three to five separate experiments and are expressed as means ± SEM; $*P < 0.05$ versus controls, ANOVA.

IEVD^{54}F (D28 and D54). Because the CCTD28N mutant exhibited greater in vitro and in vivo resistance to caspase compared with the CCTD54N mutant, it is likely that PA103 activation of caspases predominantly targets the TEED^{28}G CCTα site in pulmonary epithelial cells.

Although the molecular context by which caspases cleave CCTα in our work resemble the findings of Lagace, Miller, and Ridgway (24), there are significant functional differences between our results and their studies. Farnesol appears to activate CCTα in Chinese hamster ovary cells by relocation to the nuclear envelope, then coincident with caspase activation, CCTα is released into the cytosol; caspase proteolysis of CCTα appears to restrict the enzyme from the nuclear compartment as the nuclear localization signal is cleaved (24). In essence, despite CCTα proteolysis by caspase after farnesol exposure, the enzyme appears functional. Further, a primary feature of farnesol toxicity appears to be depletion of diacylglycerol, a substrate for CPT, thereby inhibiting PtdCho synthesis (33). In contrast, *P. aeruginosa* induces apoptosis but inhibits CCTα activity via caspase proteolysis of the enzyme. Similar to studies of calpain degradation of IκBα or CCTα, detection of caspase fragments in lung cells was not possible, presumably because of rapid clearing by endopeptidases or the proteasome (26, 34). Thus, we suspect that the CCTα proteolytic fragment, although initially intact after caspase proteolysis, undergoes additional cleavages. It is also possible that the fragment generated after caspase activation was either misfolded, exhibits altered binding affinities to its substrate, or that *P. aeruginosa* infection depletes CTP availability, all of which would render CCTα relatively less active. Because in pulmonary epithelial cells, CCTα is localized primarily in

the cytoplasm, it is unlikely that nuclear exclusion serves as an important regulatory mechanism for CCTα control (35). On the other hand, it is possible that caspase cleavage of CCTα restricts access of the enzyme to the endoplasmic reticulum or lamellar bodies, sites implicated in PtdCho synthesis in alveolar epithelia (36). Thus, significant physiologic differences exist in PtdCho metabolism for apoptosis between effects of *P. aeruginosa* infection and farnesol.

Prior studies have not addressed effects of virulence factors elaborated by *P. aeruginosa* on PtdCho synthesis. The TTSS allows pathogenic bacteria to inject bacterial proteins across the eukaryotic cell membrane directly into the cytoplasm of the host cell, thus serving as a highly effective death-effector mechanism (2, 6). We observed that toxins that emanate from the TTSS mediate cell toxicity and modulate the PtdCho biosynthetic pathway. LDH release and simultaneous cleavage of PARP serve as indicators of cytotoxicity and apoptosis, respectively, features seen after *P. aeruginosa* infection (37). PA103 mutants lacking ExoU and ExoT produced PARP cleavage similar to wild-type bacteria. Only the mutant devoid of ExoT, however, induced significant cytotoxicity, evidenced by increased LDH release and resulting in CCTα degradation (Fig. 7). These observations suggest that ExoU alone or in combination with other virulence factors is a key toxin that could inhibit the PtdCho biosynthetic pathway. Efforts directed at investigating ExoU-dependent mechanisms that suppress PtdCho production may be useful in designing newer agents to combat pulmonary infection with such virulent strains of bacteria.

This study was supported by a Merit Review Award, Department of Veteran's Affairs, The Cystic Fibrosis Foundation, and NIH R01 Grants HL-081784, HL-068135, and HL-080229 (to R.K.M.) and T32 HL-07734 (to F.C.H.). The authors thank Dr. Tim Yahr for providing PA103 mutant strains and valuable input for these studies.

REFERENCES

1. Ibrahim, E. H., S. Ward, G. Sherman, and M. H. Kollef. 2000. A comparative analysis of patients with early-onset vs late-onset nosocomial pneumonia in the ICU setting. *Chest.* **117:** 1434–1442.
2. Sadikot, R. T., T. S. Blackwell, J. W. Christman, and A. S. Prince. 2005. Pathogen-host interactions in Pseudomonas aeruginosa pneumonia. *Am. J. Respir. Crit. Care Med.* **171:** 1209–1223.
3. Meduri, G. U., R. C. Reddy, T. Stanley, and F. El-Zeky. 1998. Pneumonia in acute respiratory distress syndrome. A prospective evaluation of bilateral bronchoscopic sampling. *Am. J. Respir. Crit. Care Med.* **158:** 870–875.
4. Jenkins, C. E., A. Swiatoniowski, A. C. Issekutz, and T. J. Lin. Pseudomonas aeruginosa exotoxin A induces human mast cell apoptosis by a caspase-8 and -3-dependent mechanism. *J. Biol. Chem.* Epub ahead of print June 17, 2004;doi:10.1074/jbc.M405594200.
5. Hovey, A. K., and D. W. Frank. 1995. Analyses of the DNA-binding and transcriptional activation properties of ExsA, the transcriptional activator of the Pseudomonas aeruginosa exoenzyme S regulon. *J. Bacteriol.* **177:** 4427–4436.
6. Garrity-Ryan, L., S. Shafikhani, P. Balachandran, L. Nguyen, J. Oza, T. Jakobsen, J. Sargent, X. Fang, S. Cordwell, M. A. Matthay, et al. 2004. The ADP ribosyltransferase domain of Pseudomonas aeruginosa ExoT contributes to its biological activities. *Infect. Immun.* **72:** 546–558.
7. Goehring, U. M., G. Schmidt, K. J. Pederson, K. Aktories, and J. T. Barbieri. 1999. The N-terminal domain of Pseudomonas aeruginosa exoenzyme S is a GTPase-activating protein for Rho GTPases. *J. Biol. Chem.* **274:** 36369–36372.
8. Yahr, T. L., A. J. Vallis, M. K. Hancock, J. T. Barbieri, and D. W. Frank. 1998. ExoY, an adenylate cyclase secreted by the Pseudomonas aeruginosa type III system. *Proc. Natl. Acad. Sci. USA.* **95:** 13899–13904.
9. Sato, H., D. W. Frank, C. J. Hillard, J. B. Feix, R. R. Pankhaniya, K. Moriyama, V. Finck-Barbancon, A. Buchaklian, M. Lei, R. M. Long, et al. 2003. The mechanism of action of the Pseudomonas aeruginosa-encoded type III cytotoxin, ExoU. *EMBO J.* **22:** 2959–2969.
10. Rooney, S. A. 1985. The surfactant system and lung phospholipid biochemistry. *Am. Rev. Respir. Dis.* **131:** 439–460.
11. LeVine, A. M., K. E. Kurak, M. D. Bruno, J. M. Stark, J. A. Whitsett, and T. R. Korfhagen. 1998. Surfactant protein-A-deficient mice are susceptible to Pseudomonas aeruginosa infection. *Am. J. Respir. Cell Mol. Biol.* **19:** 700–708.
12. Malloy, J. L., R. A. Veldhuizen, B. A. Thibodeaux, R. J. O'Callaghan, and J. R. Wright. Pseudomonas aeruginosa protease IV degrades surfactant proteins and inhibits surfactant host defense and biophysical functions. *Am. J. Physiol. Lung Cell Mol. Physiol.* Epub ahead of print. October 29, 2004; doi:10.1152/ajplung.00322.2004.
13. Mariencheck, W. I., J. F. Alcorn, S. M. Palmer, and J. R. Wright. 2003. Pseudomonas aeruginosa elastase degrades surfactant proteins A and D. *Am. J. Respir. Cell Mol. Biol.* **28:** 528–537.
14. Attalah, H. L., Y. Wu, M. Alaoui-El-Azher, F. Thouron, K. Koumanov, C. Wolf, L. Brochard, A. Harf, C. Delclaux, and L. Touqui. 2003. Induction of type-IIA secretory phospholipase A2 in animal models of acute lung injury. *Eur. Respir. J.* **21:** 1040–1045.
15. Brackenbury, A. M., L. A. McCaig, L. J. Yao, R. A. Veldhuizen, and J. F. Lewis. 2004. Host response to intratracheally instilled bacteria in ventilated and nonventilated rats. *Crit. Care Med.* **32:** 2502–2507.
16. Hayashida, S., K. S. Harrod, and J. A. Whitsett. 2000. Regulation and function of CCSP during pulmonary Pseudomonas aeruginosa infection in vivo. *Am. J. Physiol. Lung Cell. Mol. Physiol.* **279:** L452–L459.
17. King, R. J., J. J. Coalson, J. J. Seidenfeld, A. R. Anzueto, D. B. Smith, and J. I. Peters. 1989. O2- and pneumonia-induced lung injury. II. Properties of pulmonary surfactant. *J. Appl. Physiol.* **67:** 357–365.
18. Qu, J., Z. Li, L. He, B. Sun, and X. Chen. 2002. Inflammatory reaction and alterations of pulmonary surfactant in Pseudomonas Aeruginosa pneumonia in immunocompromised rats. *Chin. Med. J. (Engl.).* **115:** 1099–1100.
19. Vanderzwan, J., L. McCaig, S. Mehta, M. Joseph, J. Whitsett, D. G. McCormack, and J. F. Lewis. 1998. Characterizing alterations in the pulmonary surfactant system in a rat model of Pseudomonas aeruginosa pneumonia. *Eur. Respir. J.* **12:** 1388–1396.
20. Pankhaniya, R. R., M. Tamura, L. R. Allmond, K. Moriyama, T. Ajayi, J. P. Wiener-Kronish, and T. Sawa. 2004. Pseudomonas aeruginosa causes acute lung injury via the catalytic activity of the patatin-like phospholipase domain of ExoU. *Crit. Care Med.* **32:** 2293–2299.
21. Post, M., J. J. Batenburg, E. A. Schuurmans, and L. M. Van Golde. 1982. The rate-limiting step in the biosynthesis of phosphatidylcholine by alveolar type II cells from adult rat lung. *Biochim. Biophys. Acta.* **712:** 390–394.
22. Jackowski, S., and P. Fagone. CTP:phosphocholine cytidylyltransferase: paving the way from gene to membrane. *J. Biol. Chem.* Epub ahead of print. November 9, 2004; doi:10.1074/jbc.R400031200.
23. Zhou, J., Y. Wu, F. Henderson, D. M. McCoy, R. G. Salome, S. E. McGowan, and R. K. Mallampalli. 2006. Adenoviral gene transfer of a mutant surfactant enzyme ameliorates pseudomonas-induced lung injury. *Gene Ther.* **13:** 974–985.
24. Lagace, T. A., J. R. Miller, and N. D. Ridgway. 2002. Caspase processing and nuclear export of CTP:phosphocholine cytidylyltransferase alpha during farnesol-induced apoptosis. *Mol. Cell. Biol.* **22:** 4851–4862.
25. Salome, R. G., D. M. McCoy, A. J. Ryan, and R. K. Mallampalli. 2000. Effects of intratracheal instillation of TNF-alpha on surfactant metabolism. *J. Appl. Physiol.* **88:** 10–16.
26. Mallampalli, R. K., A. J. Ryan, R. G. Salome, and S. Jackowski. 2000. Tumor necrosis factor-α inhibits expression of CTP:phosphocholine cytidylyltransferase. *J. Biol. Chem.* **275:** 9699–9708.
27. Backes, C., J. Kuentzer, H. P. Lenhof, N. Comtesse, and E. Meese. 2005. GraBCas: a bioinformatics tool for score-based prediction of

caspase- and granzyme B-cleavage sites in protein sequences. *Nucleic Acids Res.* **33:** W208–W213.
28. Kirschnek, S., and E. Gulbins. 2006. Phospholipase A2 functions in Pseudomonas aeruginosa-induced apoptosis. *Infect. Immun.* **74:** 850–860.
29. Zweigner, J., S. Jackowski, S. H. Smith, M. Van Der Merwe, J. R. Weber, and E. I. Tuomanen. 2004. Bacterial inhibition of phosphatidylcholine synthesis triggers apoptosis in the brain. *J. Exp. Med.* **200:** 99–106.
30. Holm, B. A., L. Keicher, M. Y. Liu, J. Sokolowski, and G. Enhorning. 1991. Inhibition of pulmonary surfactant function by phospholipases. *J. Appl. Physiol.* **71:** 317–321.
31. Anthony, M. L., M. Zhao, and K. M. Brindle. 1999. Inhibition of phosphatidylcholine biosynthesis following induction of apoptosis in HL-60 cells. *J. Biol. Chem.* **274:** 19686–19692.
32. Nieto-Miguel, T., C. Gajate, and F. Mollinedo. Differential targets and subcellular localization of antitumor alkyl-lysophospholipid in leukemic versus solid tumor cells. *J. Biol. Chem.* Epub ahead of print. March 15, 2006; doi:10.1074/jbc.M511251200.
33. Lagace, T. A., and N. D. Ridgway. 2005. Induction of apoptosis by lipophilic activators of CTP:phosphocholine cytidylyltransferase alpha (CCTalpha). *Biochem. J.* **392:** 449–456.
34. Han, Y., S. Weinman, I. Boldogh, R. K. Walker, and A. R. Brasier. 1999. Tumor necrosis factor-alpha-inducible IkappaBalpha proteolysis mediated by cytosolic m-calpain. A mechanism parallel to the ubiquitin-proteasome pathway for nuclear factor-kappab activation. *J. Biol. Chem.* **274:** 787–794.
35. Ridsdale, R., I. Tseu, J. Wang, and M. Post. 2001. CTP:phosphocholine cytidylyltransferase alpha is a cytosolic protein in pulmonary epithelial cells and tissues. *J. Biol. Chem.* **276:** 49148–49155.
36. Ridsdale, R., I. Tseu, M. Roth-Kleiner, J. Wang, and M. Post. Increased phosphatidylcholine production but disrupted glycogen metabolism in fetal type II cells of mice that overexpress CTP:phosphocholine cytidylyltransferase. *J. Biol. Chem.* Epub ahead of print. October 21, 2004; doi:10.1074/jbc.M407670200.
37. Jia, J., M. Alaoui-El-Azher, M. Chow, T. C. Chambers, H. Baker, and S. Jin. 2003. c-Jun NH2-terminal kinase-mediated signaling is essential for Pseudomonas aeruginosa ExoS-induced apoptosis. *Infect. Immun.* **71:** 3361–3370.